Experimental high pressure and high temperature study of the incorporation of uranium in Al-rich CaSiO$_3$ perovskite

Steeve Gréaux [a,*], Laurent Gautron [a], Denis Andrault [b,c], Nathalie Bolfan-Casanova [c], Nicolas Guignot [d,1], M. Ali Bouhifd [e]

[a] *Laboratoire des Géomatériaux et Géologie de l'Ingénieur, Université Paris-Est, 5 Bd Descartes, Champs-sur-Marne, Marne la Vallée 77454, France*
[b] *Institut de Minéralogie et de Physique des Milieux Condensés, 140 rue de Lourmel, Paris 75015, France*
[c] *Laboratoire Magmas et Volcans, Université Blaise Pascal, 5 rue Kessler, Clermont-Ferrand 63038, France*
[d] *European Synchrotron Radiation Facility, 6 rue Jules Horowitz, Grenoble 38043, France*
[e] *Department of Earth Sciences, University of Oxford, Parks Road, Oxford OX1 3PR, United Kingdom*

ARTICLE INFO

ABSTRACT

The high ability of the Al-rich CaSiO$_3$ perovskite to contain large amounts of uranium (up to 4 at.% U) has been studied up to 54 GPa and 2400 K, using laser-heated diamond anvil cell (LH-DAC) and up to 18 GPa and 2200 K using a multi-anvil press (MAP). Both latter HP-HT techniques proved to be complementary and gave similar results, in spite of different heating modes (laser and furnace). Chemical reactions were characterized and described by electron probe microanalysis and analytical scanning electron microscopy while associated structural changes were precisely characterized by synchrotron angle dispersive X-ray diffraction and by X-ray micro-diffraction.

The diffusion of uranium into the CaSiO$_3$ matrix was measured as a function of run duration and temperature. We obtain diffusion coefficients with the same order of magnitude (about 10^{-16} m^2 s^{-1}) than for those found in the literature. After this work, coupled cationic substitutions of Ca by U and Si by Al are proposed to generate new interesting crystallographic features for a CaSiO$_3$ perovskite: a higher compressibility, a tetragonal distortion along the c-axis with c/a ratio >1, a different compression behaviour of c-axis relative to a-axis, and a perovskite structure quenchable to ambient P and T conditions. The tetragonal U-bearing aluminous CaSiO$_3$ perovskite is observed to remain stable at pressures up to 54 GPa, then in the (P, T) range of the upper part of the lower mantle.

The influence of the present results, in terms of both uranium and aluminium partitioning related to the coexisting mineral phases as the (Mg,Fe)SiO$_3$ perovskite, is discussed. Uranium provides approximately 25% of the total energy generated within the deep Earth through its radioactive decay. The location of this source within the deep mantle is fundamental to the understanding of the geodynamics and thermal behaviour of our planet. Since the tetragonal structure of the U-bearing Al-rich CaSiO$_3$ perovskite is expected to remain stable towards the base of the Earth's mantle, this latter phase is proposed to be the main storage mineral for heat producing actinides of the lower mantle.

© 2008 Elsevier B.V. All rights reserved.

1. Introduction

The Earth displays clear signs of its internal activity through earthquakes, volcanic eruptions, and plate tectonics. The heat flux at the surface is of about 44 TW: 31 TW would be generated by radioactive decay of U, Th and K (6 TW from the crust, 22 TW from the mantle and about 3 TW from the core) while the remaining 13 TW would be provided by cooling of the planet by 65 K per 10^9 years (Helffrich and Wood, 2001; Kellogg et al., 1999). About 25% of the total heat production (then about 11 TW) comes from the radioactive disintegration of U through its isotopes ^{235}U and ^{238}U (Turcotte et al., 2001).

Because of its large cationic size, U is expected to partition favourably to the less-dense structures of crustal minerals rather than in the densely-packed structures found in the deep mantle. The picture is complicated, however, by the fact that the crust, which represents only a small fraction of the mantle volume, is continuously recycled into the mantle at the subduction zones. Finally, it is difficult to provide quantitative partitioning coefficients for

U between the crust and the mantle, as we hardly know which phase(s) can host uranium at the high P and T relevant to the deep Earth's mantle. In any case, it is believed that the U content in the deep mantle is not negligible. Indeed, uranium is known to be mainly present in the mantle and it is assumed that about 50 wt.% of total U in the Earth is stored in the lower mantle (Turcotte et al., 2001), which corresponds to 60,000 to 75,000 thousand millions tons of U in the lower mantle.

Our knowledge of the host minerals of uranium at P, T conditions of the mantle essentially relies on experimental studies of partitioning between solid and liquid silicates (Corgne and Wood, 2002, 2004; Tronnes and Frost, 2002; Hirose et al., 2004). The aim of these studies is to investigate the differentiation of the early mantle from the magma ocean. In a former study on the partitioning of U between majorite garnet and silicate melt at 25 GPa, Corgne and Wood (2004) showed that U acts as a highly incompatible element, i.e. U is mainly concentrated within the liquid silicate. At pressures up to 60 GPa, uranium displays the same incompatible behaviour, with very low partition coefficients between (Mg,Fe)SiO$_3$ silicate perovskite and coexisting melts (Knittle, 1998). On the other hand, another study (Corgne and Wood, 2002) revealed higher partition coefficients for U between CaSiO$_3$ perovskite and silicate melts. However those studies do not clarify whether uranium can form separate phases in the deep mantle or incorporate the main mineral phases of the lower mantle. In fact, the location of U in the solid Earth is still poorly known. However the mineralogy of uranium in the Earth's mantle is a key point to constrain the thermal and dynamic behaviour of our planet. Since uranium is known to form large cations, the incorporation of such element in deep mineral phases has also important implications in crystal chemistry and in our understanding of diffusion processes at high pressure.

Despite such major implications, only few workers have studied the mineralogy of uranium at high pressure and high temperature (Liu, 1980, 1982; Idiri et al., 2004; Wood et al., 1999; Gautron et al., 2006). Liu (1980, 1982) formerly conducted experiments on U-bearing compounds like UO$_2$ and USiO$_4$ brought to mantle P and T conditions. Liu showed that natural uraninite UO$_2$ displays a phase transformation at high pressure, which was recently identified as the transition from a fluorite-type to a cotunnite-type structure (Idiri et al., 2004); natural coffinite USiO$_4$ is shown to be unstable with pressure and decomposes into a mixture of UO$_2$ and SiO$_2$. From high P and T experiments, Wood et al. (1999) showed that the large 8-coordinated M$_2$ sites of clinopyroxenes could host uranium in the uppermost mantle. The U content in clinopyroxene appears to increase significantly with decreasing oxygen fugacity. More recently, Gautron et al. (2006) showed through HP-HT experiments, that a large amount of U (up to 35 wt.% UO$_2$) could be incorporated in the CaSiO$_3$ perovskite, at P and T relevant to the Earth's deep mantle. As proposed in a former study on a U-bearing calcium titanate CaTiO$_3$ (Hanajiri et al., 1998) and by atomic simulations (Corgne et al., 2003), the substitution of Ca^{2+} by U^{4+} in the CaSiO$_3$ perovskite could be possible thanks to the coupled substitution of two Si^{4+} by two Al^{3+}. One can note also that a monoclinic perovskite of composition CaUO$_3$ (Pialoux and Touzelin, 1998) was synthesized at room pressure and high temperatures, from mixtures of uranium dioxide and lime. But this potential host of uranium has never been observed again from HP and/or HT experiments.

Preliminary experiments (paper in preparation) revealed that MgSiO$_3$ perovskite is not able to incorporate significant amounts of uranium. Calcium is known to form the largest cation amongst the major elements present in the Earth's mantle, and as a result, it is a good candidate for a substitution by a large-radius ion like uranium. In the lower mantle, calcium is only present in the form of CaSiO$_3$ perovskite, since calcium solubility in MgSiO$_3$ perovskite is negligible (Fiquet, 2001). CaSiO$_3$ perovskite is believed to be the third most important major phase (about 7 wt.% or 5 mol%) at lower mantle conditions (Irifune, 1994; Ita and Stixrude, 1992). In the present study we propose to further constrain and fully understand the mechanism(s) of the incorporation of uranium in the high-pressure mineral phase Al-rich CaSiO$_3$ perovskite. multi-anvil press (MAP) experiments were performed in order to describe the diffusion process of the U incorporation as a function of time or temperature in the P–T stability field of the CaSiO$_3$ perovskite. Synchrotron X-ray diffraction in situ in a laser-heated diamond anvil cell (LHDAC) gave essential information about the evolution of the crystal structure of the CaSiO$_3$ perovskite related to the U incorporation, with increasing temperatures at a given pressure, and also with increasing pressures.

2. Experimental procedure

To investigate the uranium incorporation in the Al-rich Ca-perovskite, we performed HP-HT experiments on natural uraninite UO$_2$ mixed with a synthetic glass of either grossular Ca$_3$Al$_2$Si$_3$O$_{12}$ or wollastonite CaSiO$_3$ composition, in the stability field of the CaSiO$_3$ perovskite ($P > 16$ GPa, $T > 1500$ °C). The grossular glass was synthesized at 1700 °C from a mix of commercial simple oxides, and characterized by electron microprobe. This glass appears homogeneous, with the following composition in wt.%: SiO$_2$, 40.71; Al$_2$O$_3$, 21.12; CaO, 37.14. The glass of wollastonite composition was given by M. Tarrida (Université Paris-Est), as it was synthesized for former experiments (Tarrida and Richet, 1989). The composition and homogeneity of this glass was confirmed by electron probe analysis. The UO$_2$ we used as starting material is a natural uraninite from Halburton, Cardiff Township (Ontario, Canada) (sample given by J.-C. Bouillard, collection of mineralogy, Université Paris 6). Electron microprobe analyses of this material yielded a composition in wt.% as follows: UO$_2$, 89.39; ThO$_2$, 0.02; PbO, 8.06. Mixtures were prepared with excess of uranium up to 50 mol% UO$_2$, in order to enhance reactions between silicates and U-bearing compounds. We also made one HP-HT synthesis with a mix of simple oxides: CaO, SiO$_2$, Al$_2$O$_3$ and UO$_2$ with the same stoichiometry as in the mix of grossular + UO$_2$.

HP-HT experiments were done in a 1000-ton MAP (French national facility, Clermont-Ferrand) and a membrane-type LHDAC available at the European Synchrotron Radiation Facility (ESRF, Grenoble). Multi-anvil press experiments were conducted within 10/4 assemblies: Cr-doped MgO octahedron, side-length = 4 mm; WC truncation edge-length = 10 mm, supported by pyrophilite gaskets. Powder of the starting material was enclosed in a Pt capsule, and a LaCrO$_3$ furnace was used to supply heating. Experimental conditions and pressure calibrations in the multi-anvil experiments were similar to those described previously (Rubie, 1999; Hammouda, 2003). The procedure used with the diamond anvil cell is reported elsewhere (Andrault and Fiquet, 2001). No heating agent was used in the DAC as uraninite appeared to absorb the YAG laser radiation very well. Argon was used as soft pressure medium in order to minimize deviatoric stresses that can develop during compression.

Multi-anvil samples are quenched to room temperature then brought back to ambient pressure. After being recovered, they were encapsulated in epoxy resin for analysis. For all samples, the chemical analysis from the high pressure phases were obtained by using an Electron Probe Micro-Analysis (EPMA; LMV, Clermont Ferrand; CCR, Université Paris 6) while imaging and additional micro-analysis were also performed with a Leo Stereoscan 440 analytical scanning electron microscope (ASEM; LISE, Université

Table 1
Experimental conditions and results for multi-anvil press (MAP) runs

Conditions (P, T, runtime)		Average[+] composition (in wt.%) for the Ca-Pv with standard deviation				Accessory phases
		CaO	SiO_2	Al_2O_3	UO_2	
$CaSiO_3$ (Wol.) + UO_2						
MA-250	18 GPa, 2000 K, 3 h	37.1 (2.4)	61.8 (2.0)	–	0.8 (0.7)[*]	UO_2
$CaSiO_3$ (Wol.) + UO_2 + Al_2O_3						
MA-265	18 GPa, 2000 K, 3 h	33.4 (4.4)	31.3 (4.7)	10.6 (1.7)	22.3 (5.0)	SiO_2, CAS, UO_2
MA-324	18 GPa, 2000 K, 12 h	30.8 (2.3)	29.1 (3.1)	13.8 (1.7)	26.4 (4.4)	SiO_2, CAS, UO_2
$Ca_3Al_2Si_3O_{12}$ (Gro.) + UO_2						
MA-249	18 GPa, 2200 K, 20 s	32.6 (5.4)	28.9 (7.7)	12.0 (3.7)	26.4 (10.2)	SiO_2, CAS, UO_2
MA-251	18 GPa, 2000 K, 3 h	34.2 (2.3)	31.2 (3.3)	11.2 (1.6)	23.7 (3.8)	SiO_2, CAS, UO_2
MA-312	18 GPa, 2000 K, 8 h	29.4 (1.4)	25.5 (2.1)	15.0 (1.1)	29.9 (2.9)	SiO_2, CAS, UO_2
MA-323	18 GPa, 2000 K, 12 h	29.9 (1.3)	26.9 (1.4)	14.0 (0.6)	28.8 (1.3)	SiO_2, CAS, UO_2
$Ca_3Al_2Si_3O_{12}$ (Gro.) + UO_2 + Al_2O_3						
MA-266	18 GPa, 2200 K, 3 h	33.1 (0.0)	28.8 (1.2)	12.2 (0.0)	25.7 (0.2)	SiO_2, CAS, UO_2, Al_2O_3
$CaO + SiO_2 + Al_2O_3 + UO_2$						
MA-265	18 GPa, 2000 K, 3 h	31.4	30.3	14.4	23.4	SiO_2, CAS, UO_2

Wol. = wollastonite; Gro. = grossular.
Ca-Pv = $CaSiO_3$ phase with a perovskite structure (evidenced by μ-XRD on samples MA-312 and MA-323). CAS = CAS phase of composition $CaAl_4Si_2O_{11}$.
[+] Average composition is calculated for about 10 analyses in homogeneous areas (i.e. far from "diffusion" cells).
[*] This value is within the error bar of the analysis technique: Fig. 1a shows that there is no U in the Ca-Pv observed in sample MA-250.

Paris 6) equipped with a Princeton Gamma-Tech (PGT) spirit energy-dispersive X-ray analyzer (EDX). Duration of analyses was of about 100 s for each analysis, and one second per point for quantitative composition maps. Composition profiles could be obtained to constrain the diffusion processes that occurred in the HP samples. Details and conditions of the multi-anvil experiments as well as the chemical analyses of the quenched samples are listed in Table 1. X-ray micro-diffraction measurements were performed on some multi-anvil samples, in the Application Support Department of Bruker Nonius BV (Delft, The Netherlands). Regions of interest were located by using a laser-video microscope (resolution to 50 μm), and analyzed with a D8 discover diffractometer system (equipped with a two-dimensional HI-STAR detector); the duration was typically about 1 h. The phase identification was achieved by using the *DIFFRAC^{plus} SEARCH* search/match procedure of the *GADDS* software (Caussin et al., 1988).

Diamond anvil cell experiments were carried on a mix of grossular glass and uranium oxide. Starting materials were exactly the same as those used for the MAP samples MA-312 and MA-323 (see Table 1). Two runs were performed in order to investigate the structure of the U-bearing Al-$CaSiO_3$ phase under high-pressure and high-temperature conditions: firstly at 23 GPa with temperature varying from 1800 to 2400 K (run DAC-01); secondly from 31 GPa to 54 GPa with annealing at about 2400 K after each step of compression (run DAC-02). Samples were analyzed in situ by angle dispersive X-ray diffraction performed at the insertion device ID30 (now ID27) at the European Synchrotron Radiation Facility (ESRF). A water-cooled Si(1 1 1) bent Laue monochromator was used to produce a bright monochromatic X-ray beam at a wavelength of 0.3738 Å. Vertical and horizontal focusing were achieved with a spherical mirror and a monochromator respectively. The X-ray flux on a 15-by-15 μm spot allowed the acquisition of diffraction patterns on an imaging plate within about 5 min. The two dimensional images were integrated to one-dimensional two-theta scans with the Fit2d code (Hammersley et al., 1996). Lebail and Rietveld profile refinements of the structure were applied with the program package *GSAS/EXPGUI* (Larson and Von Dreele, 1994; Toby, 2001) in order to extract cell parameters and volumes for all high-pressure phases.

3. Results

3.1. Multi-anvil press results

In all multi-anvil samples synthesized in the system U–Ca–Al–Si–O, we observed a U-bearing phase of stoichiometry $CaSiO_3$ as described by Gautron et al. (2006). This phase, which was the major phase of our samples, was observed and analyzed by electron probe micro-analysis (EPMA) and analytical scanning electron microscopy (ASEM) (see Fig. 1). The incorporation of uranium in the $CaSiO_3$ phase was coupled to the formation of accessory phases like the CAS phase of composition $CaAl_4Si_2O_{11}$ (Gautron et al., 1996) and stishovite SiO_2 (Fig. 1). In all our samples we could find some small amounts of remaining UO_2 grains, indicating that U can be inserted into the $CaSiO_3$ phase up to a definite amount. Moreover, when Al_2O_3 is added to the $CaSiO_3$ starting glass, there is still some Al_2O_3 left among the experimental products (run MA-324). The presence of Al in the system seems to be the key point for the diffusion of U: indeed, as shown in Fig. 1b, no uranium enters the $CaSiO_3$ phase in sample MA-250, where there is no aluminium in the starting material.

Further investigation of the U–Ca–Al–Si–O system as a function of time (see Fig. 2) and temperature showed that a diffusion process controls the incorporation of U. All the starting systems we used (with wollastonite, grossular or oxides mix) displayed similar reactions that were enhanced by time duration and temperature. We observed similar reactions and results (with grossular as starting material) in the 20 s-run at 2200 K (MA-249) and in the 3 h-run at 2000 K (MA-251). In another 3 h-run (MA-265, with wollastonite as starting material), we observe that the diffusion of U from a UO_2 grain to the Al-$CaSiO_3$ phase is not achieved. Note that when aluminium is present but not in the starting silicate material (MA-265), slightly less uranium can be incorporated in the Ca-perovskite. Fig. 2a displays a zone around a grain of UO_2 (sample MA-265), which could be described as a diffusion cell. In such zone, the U content of the Al-$CaSiO_3$ phase can vary by 3 at.% between parts close and far from the UO_2 grain. We obtained various profiles of composition from regions of interest like the diffusion cell described above. Diffusion in these experiments could be described by the equation for one-dimensional diffusion in a semi-infinite medium,
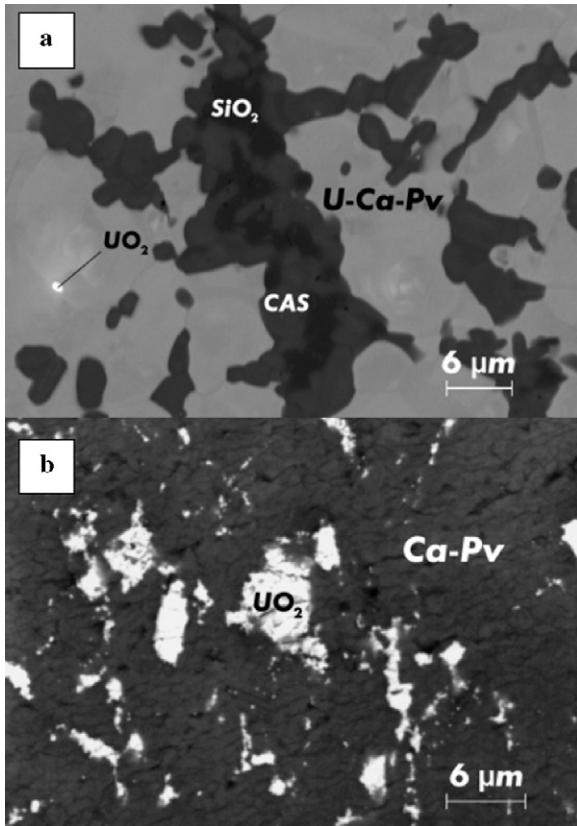
Fig. 1. Backscattered electron image of the MA-250 and MA-251 samples synthesized at 18 GPa and 2000 K for 3 h. (a) The U-bearing Al-rich $CaSiO_3$ (UCa-Pv) is the major phase of the sample MA-251. In addition to this phase, we observed the CAS phase ($CaAl_4Si_2O_{11}$), SiO_2 stishovite (St) and a small amount of UO_2. (b) There was no reaction between UO_2 and $CaSiO_3$ when no Al is present in the starting materials (sample MA-251).

with constant interface concentration:

$$\frac{C(x,t) - C_0}{C_i - C_0} = \text{erf}\left[\frac{x}{2(Dt)^{0.5}}\right] \tag{1}$$

where $C(x,t)$ is the concentration at depth x after annealing time t, C_0 is the concentration at the interface, C_i is the initial concentration in the $CaSiO_3$ perovskite (essentially zero for U), and D is the diffusion coefficient. A typical diffusion profile is shown in Fig. 3. To extract a diffusion coefficient from the data, each profile is linearized by plotting the inverse error function of the left-hand side of Eq. (1) against depth x. We obtain a diffusion coefficient of uranium in the Al-$CaSiO_3$ perovskite, $D_{U/Al-Capv} = 1.6$–1.8×10^{-16} m^2 s^{-1}. This value appears quite high compared to the values of diffusion coefficient of uranium in diopside ($D_{U/diopside}$ around 10^{-20} m^2 s^{-1}, Van Orman et al., 1998). However, the values are very similar to those obtained by Seitz (1973), who reported a U tracer diffusion coefficient for diopside of 10^{-16} m^2 s^{-1} at 1240 °C. In fact our experiments are comparable to those performed by Seitz (1973), since in both cases growth of crystals during experiments is expected to enhance the diffusion of uranium, and then to generate high diffusion coefficients. It appears clear that from the present work, crystals of Ca-perovskite were growing in parallel to the diffusion of U into these crystals.

We observed larger grains for the 8 h-run MA-312 with a greater homogeneity (Fig. 2b) and a U content of the Al-$CaSiO_3$ phase up to 4 at.%. The U-bearing Al-$CaSiO_3$ grains kept growing up to 12 h as seen in MA-323 (Fig. 2c): empty spaces between the grains of the U–Al $CaSiO_3$ phase were reduced between 8 h and 12 h, and grain
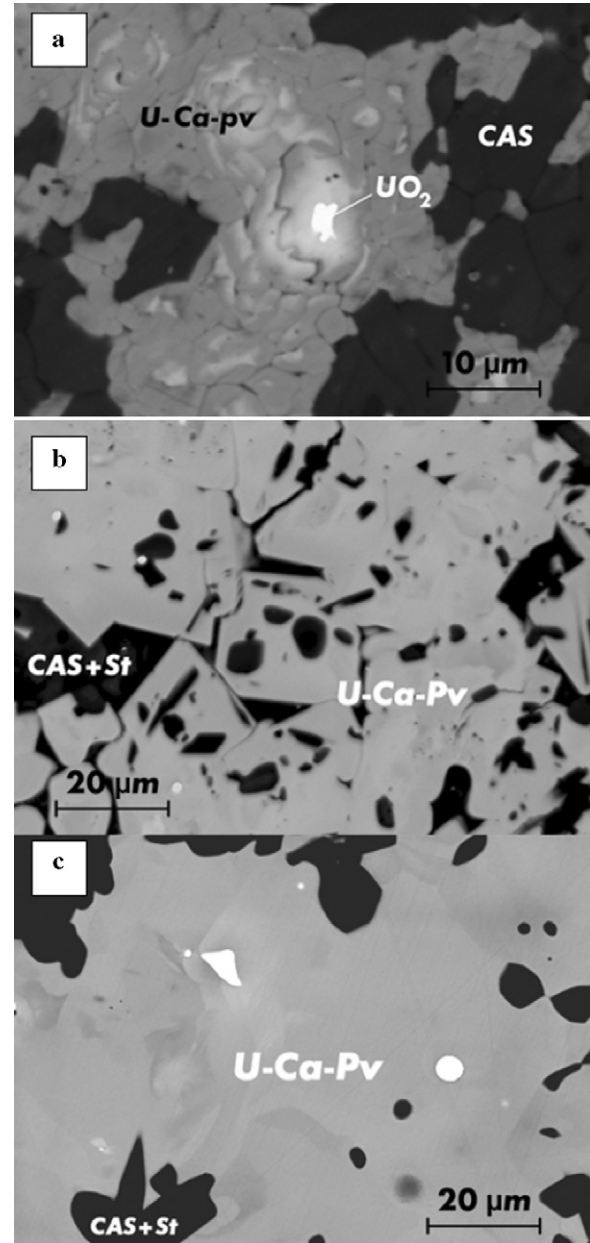
Fig. 2. Backscattered electron images of the MA-251, MA-312 and MA-323 samples synthesized at 18 GPa and 2000 K for respectively 3, 8 and 12 h (respectively Fig. 2a, b and c). The incorporation of U follows a diffusion process and is influenced by run duration and temperature. The grains keep growing up to 12 h duration but the maximum amount of U (35 wt.% UO_2) that can be incorporated in the $CaSiO_3$ perovskite, is already reached after 8 h.

boundaries were more difficult to detect after 12 h. But we observed no change in the U content of the Al-$CaSiO_3$ phase in comparison with the 8 h-run. This feature indicates that the incorporation of U in the $CaSiO_3$ phase is completed after few hours: then the later phase would display a saturation of uranium, since there was still some UO_2 left after 8 or 12 h of run duration (see Table 1). The electron probe micro analysis (EPMA) of all our HP samples showed an average incorporation of U in the $CaSiO_3$ high-pressure phase of about 22–30 wt.% of UO_2, with the highest rate yielded by the phase in MA-312, as follow (in wt.%): CaO, 29.4; SiO_2, 25.5; Al_2O_3, 15.0; UO_2, 29.9.

A recent X-ray absorption study by Gréaux et al. (2007) revealed that uranium presents a 4+ oxidation state in the U-bearing Al-
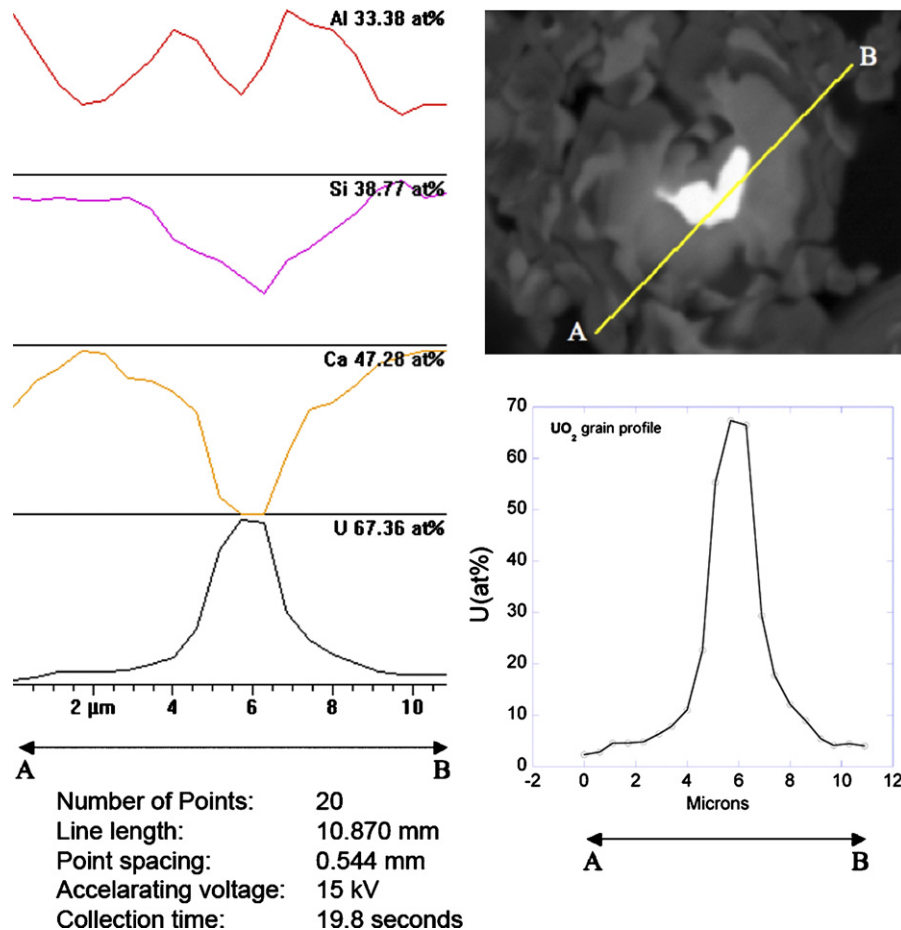
Fig. 3. Example of a diffusion profile obtained from EDX-ASEM analysis on sample MA-265. The profile was performed from point A to point B (distance = 10.87 μm), with a total of 20 points (1 analysis per point). This profile goes through the "diffusion cell" of uranium from the UO_2 grain to the Al-$CaSiO_3$ surrounding phase. The detailed profile for each element (Al, Si, Ca, U) is labelled with the maximum content (values in at.% displayed at the top right of each profile) obtained for the profile. A more precise profile for uranium is presented at the bottom right of this figure.

$CaSiO_3$ phase: this result indicates that both multi-anvil press and diamond anvil cell experiments generate rather reducing conditions (or at least non-oxidizing). As observed for clinopyroxene (Wood et al., 1999), the U content of the Al–Ca-perovskite could be increased under such experimental conditions with a lower oxygen fugacity Based on steric considerations, uranium is expected to enter the dodecahedral calcium site in the $CaSiO_3$ phase since U^{4+} and Ca^{2+} display similar ionic radii: 1.17 Å and 1.34 Å respectively when 12-fold coordinated (Shannon, 1976). Based on stoichiometry obtained from EPMA analyses, Gautron et al. (2006) proposed that Al should be present not only in the Si site but also in the Ca site (see Andrault et al., 1998), then formulated the U-bearing Al-$CaSiO_3$ as follows: $(Ca_{0.795}, U_{0.200}, Al_{0.005})(Si_{0.595}, Al_{0.405})O_3$. Note that if we just consider stoichiometry given by chemical analyses, the U-bearing Al-$CaSiO_3$ phase displays the exact amounts of U and Al corresponding to the substitution of Ca by U charge balanced by the substitution of Si by Al. Micro-analyses showed that lead, which is present in the composition of the starting material uraninite UO_2, clearly partitions in favour of the CAS phase. Then we can assume that the lead initially incorporated in the system has no influence on the chemical reactions observed in this study, and no effect on the crystal structure of the U-bearing Al-$CaSiO_3$ perovskite.

X-ray micro-diffraction was performed on 50–100 μm square regions of U-bearing Al-$CaSiO_3$ in samples MA-312 and MA-323. We selected a zone with no UO_2 grain but the platinum casing material was still too close so that some Pt reflections were present in the XRD patterns. The GADDS search/match routines revealed that both samples displayed the same assemblage: stishovite SiO_2, CAS phase ($CaAl_4Si_2O_{11}$) and peaks which could be attributed to a U-bearing $CaSiO_3$ phase as observed and analyzed by EPMA and ASEM. Fig. 4 displays a typical X-ray microdiffraction pattern of the assemblage obtained in this study. The diffraction lines of the U-bearing $CaSiO_3$ phase can be explained by a tetragonal symmetry, within the $P4/mmm$ space group with $a_0 = 3.6345(2)$ Å and $c_0 = 3.6638(4)$ Å, $V_0 = 48.397(6)$ Å^3. This structure displays a slight distortion from a cubic perovskite. Such distortion for the $CaSiO_3$ perovskite at P, T conditions of the deep mantle, was predicted by calculations (Stixrude et al., 1996; Jung and Oganov, 2005; Caracas et al., 2005; Caracas and Wentzcovitch, 2006). This HP-HT crystal structure of the Ca-perovskite was confirmed by numerous experimental in situ measurements, which have been performed on $CaSiO_3$ perovskite under high pressure (Wang et al., 1996; Shim et al., 2000a,b, 2002).

The room-pressure recovering of the high-pressure crystal structure of the Ca-perovskite is an unexpected feature since the $CaSiO_3$ perovskite is known to be commonly unquenchable and to bear an amorphization when quenched to ambient conditions (as first found by Liu and Ringwood (1975)). Other studies (Yusa et al., 1995; Takafuji et al., 2002; Kurashina et al., 2004) described the influence of aluminium and/or high temperatures on the crystal structure evolution of the $CaSiO_3$ perovskite. These works clearly showed that above a lower limit in the Al content, part of the HP crystallized assemblage could be quenchable: with
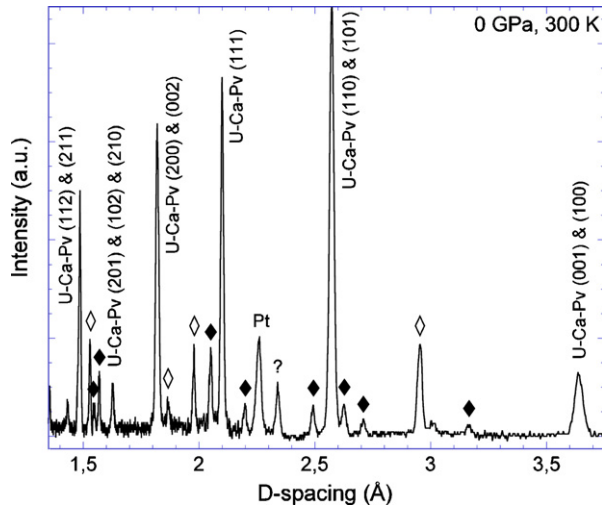
Fig. 4. X-ray micro-diffraction spectra recorded at room conditions on a 100 μm square region in sample MA-312 synthesized at 18 GPa and 2000 K for 8 h. The identification and indexation of the phases were done by using the *GADDS* software. The U-bearing Al-CaSiO$_3$ diffraction lines are explained by a tetragonal symmetry, with a space group *P4/mmm*. Rietveld refinement yielded the cell parameters as follows: $a_0 = 3.6345(2)$ Å and $c_0 = 3.6638(4)$ Å. The black and white diamonds represents respectively the diffraction lines of CAS phase (CaAl$_4$Si$_2$O$_{11}$) and those of SiO$_2$ stishovite (St). There is also one unidentified peak (labelled with (?)) and a peak of Pt that we used as the casing material in MAP experiments.

Fig. 5. Synchrotron angle dispersive X-ray diffraction patterns recorded for the DAC-01 sample at 23 GPa, with increasing temperature from 1800 to 2400 K at ESRF's ID30 beamline (now ID27). The diamond anvil cell sample was heated by making successive annealing on both sides by using two YAG lasers. For low temperature measurements, Rietveld structure refinements show argon (pressure transmitting medium), fluorite-type UO$_2$, CaSiO$_3$ perovskite as the main phases. With increasing temperature of heating, UO$_2$ and CaSiO$_3$ perovskite lines disappear and a U-bearing Al-rich CaSiO$_3$ tetragonal perovskite phase (U-Ca-Pv) appears for annealing temperatures from 2000 to 2400 K. SiO$_2$ stishovite is present in this range of pressure and temperature, and we can not exclude the presence of the CaAl$_4$Si$_2$O$_{11}$ (CAS) phase observed in the multi-anvil samples.

Al content up to 6 mol%, a mix of amorphous CaSiO$_3$ and crystalline Al$_2$O$_3$ is observed (Takafuji et al., 2002). The same study reported that Al-CaSiO$_3$ with 8–25 mol% of Al$_2$O$_3$ also transforms to an assemblage of alternating lamellae of amorphous layer and LiNbO$_3$-type phase. Asahara et al. (2005) reported the occurrence of a CaSiO$_3$ perovskite which incorporates Mg, Fe and Al to form a Ca(Mg,Fe,Al)Si$_2$O$_6$ perovskite at HP-HT. Due to the metastable nature of this phase, only a mix of an amorphous CaSiO$_3$ phase and Al-bearing (Mg,Fe)SiO$_3$ could be observed in their quench products. The Al-CaSiO$_3$ phase with a perovskite structure observed in the present study incorporates large amounts of uranium (about 35 wt.% of UO$_2$) and aluminium (nearly 13 wt.% of Al$_2$O$_3$). Then, unlike the other Ca-perovskite phases described above, the U-bearing Al-CaSiO$_3$ perovskite appears to be quenchable to ambient pressure conditions and we can observe large grains of this phase (up to 20–30 μm large), as seen in Fig. 2b and c.

3.2. Diamond anvil cell results

The crystal structure of the U-bearing CaSiO$_3$ phase was investigated by X-ray diffraction with synchrotron radiation, realized *in situ* at HP-HT in a LHDAC. Fig. 5 shows the evolution of the diffraction pattern for the mixture of grossular and uraninite at 23 GPa, as a function of temperature. At this pressure, UO$_2$ displays a fluorite structure and the grossular is found to transform to a CaSiO$_3$ phase with a perovskite structure. Despite extensive examination, we found no indication that Al$_2$O$_3$ was released: thus we assumed that the initial aluminium is present in the final products of the reaction: the CaSiO$_3$ perovskite, but also in the expected accessory phase (the CAS phase and in a less extent stishovite). The other lines are from argon, used as pressure transmitting medium in the diamond anvil cell. When we increase temperature, we observe that the diffraction lines of UO$_2$ and CaSiO$_3$ perovskite clearly decrease from 1800 to 2200 K. In the same range of temperatures, we observe new diffraction lines increasing besides those from the CaSiO$_3$ perovskite. At 2400 K, there is no more UO$_2$ and CaSiO$_3$ but a U-bearing phase that have incorporated all the uranium of the starting mate-

rial. Such progressive incorporation of U in the Ca-perovskite when increasing temperature is in good accordance with the observations on quenched MAP samples as a function of time (as presented in Fig. 2).

We recorded X-ray diffraction patterns *in situ* while heating in the DAC and after temperature quench of the U-bearing Ca-perovskite phase, as a function of pressure from 31 to 54 GPa (Fig. 6). Rietveld and Lebail refinement were performed on all *in situ* measurements: the major diffraction lines from all patterns could be explained by a mix of argon and a U-bearing aluminous Ca-perovskite with the same stoichiometry as the U-bearing CaSiO$_3$ phase observed and characterized by EPMA and ASEM in the multi-anvil samples. According to the MAP observations, the presence of CAS in our DAC samples is plausible but could not be evidenced from the X-ray diffraction patterns. The CAS phase is only present as small amounts (as shown by the MAP results) and is characterized by a lower symmetry (Gautron et al., 1999): then lines from the CAS phase are expected to be very weak compared to those of coexisting phases. Lines from SiO$_2$ stishovite may also be present but for similar reasons as for the CAS phase could not be clearly observed in the current work.

Table 2 lists the atomic positions used for the Rietveld analysis of the U-bearing Al-CaSiO$_3$ perovskite: we used the site occupancies corresponding to the stoichiometry evidenced by EPMA and ASEM analyses on MAP samples. All the diffraction peaks obtained from the U-bearing Ca-perovskite could be indexed within the *P4/mmm* (1 2 3) tetragonal symmetry ($Z = 1$), as first described by Gautron et al. (2006): this result confirms the μ-XRD results obtained on the same phase synthesized in a multi-anvil press. Table 3 presents the detail of the refinement for the X-ray diffraction at 31 GPa. The agreement factors obtained from the Rietveld refinement at all pressures were in the range 1–5% for R_{wp} and R_p, and in the range
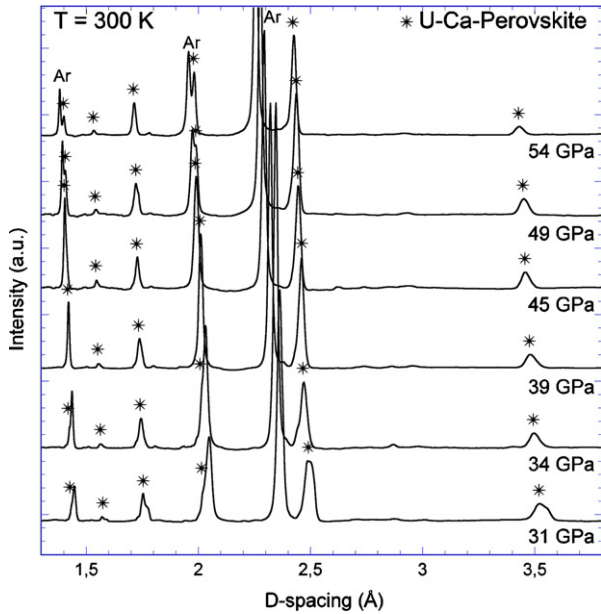
Fig. 6. Several synchrotron angle dispersive X-ray diffraction patterns recorded for the DAC-02 sample as a function of pressure. The diamond anvil cell sample was heated by making successive annealing on both sides after each compression step by using two YAG lasers. Rietveld structure refinements on these phases show no phase transition from 31 to 54 GPa. The tetragonal U-bearing Al-CaSiO$_3$ perovskite remains stable at pressures up to 54 GPa.

Table 2
Atomic positions and site occupancies for the U-bearing Al-rich CaSiO$_3$ perovskite, as used for Rietveld refinements

Space group: $P4/mmm$; $Z = 1$						
Atom	m	w	x/a	y/b	z/c	Occupancy
Ca	1	a	0	0	0	0.795
U	1	a	0	0	0	0.200
Al1	1	a	0	0	0	0.005
Si	1	d	0.5	0.5	0.5	0.595
Al2	1	d	0.5	0.5	0.5	0.405
O1	1	c	0.5	0.5	0	1.000
O2	2	e	0	0.5	0.5	1.000

m and w correspond to the multiplicity and the Wyckoff notation respectively.

1–3 for χ^2. These values indicate that we could perform accurate Rietveld refinements of our XRD data at each pressure.

Table 4 lists cell parameters, c/a values and volumes of the U-bearing CaSiO$_3$ perovskite at all pressures during compression and decompression as well. We see that the c/a ratio is relatively constant; furthermore there is no significant difference between the c/a ratios from 31 to 54 GPa (average value of 1.008 with a stan-

Table 3
Results from the structure refinement of the U-bearing Al-CaSiO$_3$ perovskite at 31 GPa; $a = 3.4999(6)$ Å, $c = 3.5419(9)$ Å, $V = 43.385(15)$ Å^3, space group $P4/mmm$, $Z = 1$

d_{hkl} (Å)	I_{obs}	I_{calc}	$h\,k\,l$
3.5599	22	16	0 0 1
3.5072	25	18	1 0 0
2.4984	100	100	1 0 1
2.4800	97	93	1 1 0
2.0349	46	39	1 1 1
1.7800	23	21	0 0 2
1.7536	43	36	2 0 0
1.5873	3	4	1 0 2
1.5731	6	5	2 0 1
1.5685	7	5	2 1 0

Agreement factors: $R_{wp} = 2.88\%$; $R_p = 1.39\%$; $\chi^2 = 1.686$.

Table 4
Refined unit-cell parameters and volume for the U-bearing Al-CaSiO$_3$ perovskite as a function of pressure

P (GPa)	a (Å)	c (Å)	c/a	V (Å^3)
31.3(3)	3.4999(6)	3.5419(9)	1.012	43.385(15)
32.3(3)	3.4909(6)	3.5237(10)	1.009	42.943(14)
32.6(3)	3.4934(6)	3.5240(10)	1.009	43.009(14)
34.4(3)	3.4857(7)	3.5137(12)	1.008	42.694(17)
34.7(3)	3.4852(6)	3.5150(9)	1.008	42.696(14)
34.8(3)	3.4847(4)	3.5107(7)	1.007	42.633(10)
39.0(4)	3.4773(6)	3.4981(9)	1.006	42.298(13)
45.0(4)	3.4516(4)	3.4761(7)	1.007	41.415(9)
49.0(5)	3.4417(5)	3.4650(8)	1.007	41.044(13)
50.4(5)	3.4363(4)	3.4628(7)	1.008	40.892(9)
54.2(5)	3.4261(6)	3.4458(10)	1.006	40.449(12)
44.9 (5)[*]	3.4529(6)	3.4710(9)	1.005	41.385(14)
38.3(4)[*]	3.4677(5)	3.4968(10)	1.008	42.051(13)
32.1(3)[*]	3.4973(5)	3.5239(9)	1.008	43.103(13)
26.6(3)[*]	3.5149(8)	3.5434(13)	1.008	43.779(18)
0.0[*]	3.6386(4)	3.6652(2)	1.007	48.527(12)

[*] Values obtained from spectra upon decompression.

dard deviation of 0.001) and the c_0/a_0 ratio (1.008) calculated for the quenched U-bearing Al-CaSiO$_3$ phase in the MAP sample. Liu and Ringwood (1975) showed that CaSiO$_3$ crystallizes in the cubic Pm3m perovskite structure at 16 GPa and 1800 K but a tetragonal distortion with an axis ratio c/a 0.4 to 0.7% different from that of the cubic structure has been proposed and observed as being the stable structure of CaSiO$_3$ perovskite at mantle conditions (Stixrude et al., 1996; Shim et al., 2002). Unlike pure CaSiO$_3$ perovskite where c-axis is shorter than a-axis, the U-bearing Al–Ca-perovskite observed in our experiments, presents a c-axis about 0.9% longer than the a-axis. Note also that the c-axis of the U–Al Ca-perovskite appears about 12% more compressible than the a-axis (after the data listed in Table 4), while pure tetragonal Ca-perovskite would present a c-axis 5 to 6% less compressible than the a-axis (Shim et al., 2002). These discrepancies could be due to the presence of uranium and aluminium together in the Ca-perovskite.

The incorporation of aluminium in the Ca-perovskite structure has been studied recently at HP-HT (Kurashina et al., 2004). They reported that, at low temperatures, CaSiO$_3$ perovskite with an Al content of about 5.9 mol% displays an orthorhombic structure while the Al-free CaSiO$_3$ perovskite is tetragonal as observed in former studies mentioned above. With increasing temperatures, both Al-bearing and Al-free CaSiO$_3$ perovskites appear to adopt a cubic structure, as observed and predicted in various former studies (Stixrude et al., 1996; Akber-Knutson et al., 2002; Kurashina et al., 2004; Komabayashi et al., 2007). These phase transitions are proposed to explain some seismic discontinuities in the range of 700–1800 km depth. In our study, with increasing P and T, we did not see a progressive transition from a tetragonal to a cubic structure. The U-bearing Al-CaSiO$_3$ perovskite observed in this study keeps displaying a tetragonal symmetry at pressures up to 54 GPa. The discrepancy between the results of this work and those from Kurashina et al. (2004) could be due to the high Al content in the U-bearing Al-CaSiO$_3$ perovskite (11.25 mol% Al$_2$O$_3$), nearly twice the Al content presented by Kurashina et al. (2004): such high Al content could slow or stop any transition towards a cubic structure. But another explanation could be found with the substitution of Ca by U: more work is clearly needed to understand such behaviour and mechanism.

The U-bearing aluminous CaSiO$_3$ perovskite remains stable at pressures up to 54 GPa, then in the (P, T) range of the upper part of the lower mantle. Third-order Birch–Murnaghan equation of state for the compression curve of the U-bearing CaSiO$_3$ perovskite was calculated elsewhere (Gautron et al., 2006). Table 5 lists the EOS

Table 5
EOS parameters of Al-free and Al-bearing CaSiO$_3$ perovskites, compared to those of the U-bearing Al-rich CaSiO$_3$ perovskite

Phase	K_0 (GPa)	K_0'	V_0 (Å^3)	Reference
U-Ca-Pv (DAC)	219(6)	3.4(3)	48.527(12)	Gautron et al. (2006)
Orthorhombic Ca-Pv	228(2)	4.3(1)	45.90(2)	Akber-Knutson et al. (2002)
Tetragonal Ca-Pv	255(5)	4.0[*]	45.58[**]	Shim et al. (2002)
Cubic Ca-pv	236(4)	3.9(2)	45.58(5)	Shim et al. (2000a,b)
Cubic Ca-Pv	232(8)	4.8(3)	45.58(4)	Wang et al. (1996)
Orthorhombic Al-Ca-Pv	283(7)	4.0[*]	45.99	Yusa et al. (1995)

[*] Fixed value for the pressure derivative of the bulk modulus.
[**] Fixed value for the volume at ambient conditions, from Wang et al. (1996).

parameters of various Ca-perovskites from the literature. The first pressure derivative of the bulk modulus obtained by Gautron et al. (2006) ($K_0' = 3.4 \pm 0.3$) is slightly smaller than those calculated for pure CaSiO$_3$ perovskite ($K_0' = 4.3 \pm 0.1$ from Akber-Knutson et al. (2002); $K_0' = 3.9 \pm 0.2$ from Shim et al., 2000a,b; $K_0' = 4.8 \pm 0.3$ from Wang et al. (1996)). Nevertheless, the value of $K_0' = 3.4 \pm 0.3$ yielded by Gautron et al. (2006) is rational for a mineral of the Earth's lower mantle. In fact, the experimental values of K_0' for many close-packed minerals are usually close to 4 (Poirier, 2000).

The bulk modulus calculated for the U-bearing CaSiO$_3$ perovskite ($K_0 = 219 \pm 6$ GPa; after the PV EOS from Gautron et al. (2006)) is significantly smaller than those determined for pure CaSiO$_3$ perovskite ($K_0 = 236 \pm 4$ GPa after the PVT EOS from Shim et al. (2000a,b); $K_0 = 228 \pm 2$ GPa after the PV EOS from Akber-Knutson et al. (2002); $K_0 = 232 \pm 8$ GPa after the PVT EOS from Wang et al. (1996); $K_0 = 255 \pm 5$ GPa after EOS from Shim et al. (2002)). The zero-pressure volume of the U–Al Ca-perovskite is at least 5% larger than those obtained for all other CaSiO$_3$ perovskites (Table 5). Thus, the U-bearing Al-rich Ca-perovskite would be about 4–14% more compressible than pure Ca-perovskite. One can note that Yusa et al. (1995) reported an even less compressible ($K_0 = 283 \pm 7$ GPa) Al-rich Ca-perovskite with a grossular composition (Ca$_3$Al$_2$Si$_3$O$_{12}$, then 22.6 wt.% Al$_2$O$_3$). Cationic substitutions clearly have a major influence on compressibilities of high pressure minerals: for example, magnesium silicate perovskite containing 5 mol% Al$_2$O$_3$ was found to be about 10% more compressible than pure magnesium end-member perovskite (Zhang and Weidner, 1999). In the same way, the relatively high Al content (12.65 wt.% Al$_2$O$_3$ or 7.30 at.% Al) of the U-bearing CaSiO$_3$ perovskite would contribute to increase its compressibility. Note that the bulk modulus of the U–Al bearing Ca-perovskite is the lowest ever reported for a CaSiO$_3$ perovskite. Then in addition to the effect of Al, the incorporation of uranium could make the Ca-perovskite even more compressible.

4. Discussion

This experimental study shows that large-radius cations like those of uranium can be incorporated as large amounts into mantle silicates via a diffusion process: as expected, this process is activated by high temperatures and/or long run durations, but it appears that there is no negative effect of high pressure. Indeed, pressure is known to lower the diffusion coefficients (Poirier, 2000): but after the results we obtained in this study, we can assume that the effect of temperature was substantially more important than the effect of pressure, and high temperatures combined with long run durations could efficiently activate the diffusion process of the U incorporation at high P. We obtained diffusion coefficients for U into the Al-CaSiO$_3$ perovskite at high P and T, in the same order of magnitude than those of U into diopside observed at high T: our experiments could not be considered as so-called diffusion experiments (like those described in the review by Béjina et al., 2003),

but they allowed us to quantify the effect of both run duration and temperature on the diffusion process of uranium into the Al-CaSiO$_3$ perovskite. Two other characteristics are also essential for such diffusion: the size and the charge of the cation diffusing into the Ca-perovskite matrix. In fact, U^{4+} is slightly smaller than Ca^{2+}, and furthermore its charge is twice bigger: these two arguments are in favour of the relatively easy diffusion of uranium at high P and T, that we could observe in this study.

The aluminium plays a key role in the diffusion process of uranium into a mantle silicate mineral, as we showed that without aluminium into the starting material, no uranium at all could enter the CaSiO$_3$ perovskite. The charge compensation appears to be the central point for the incorporation of cations with a valence higher than that of the cations that they replaced. The substitution of 2 Si^{4+} by 2 Al^{3+} was observed in various former works (Madon et al., 1989; Gautron and Madon, 1994). The present experiments further evidence that such substitution can be coupled to that of one Ca^{2+} by one U^{4+}, to allow the charge compensation, as proposed by former studies (Corgne et al., 2003; Gautron et al., 2006). Such mechanism could be rather complex since the substitution occurring into one site (the Si site) has a direct influence to the possibility of substitution into another site (the Ca site). This feature is essential for this incorporation of uranium into the Al-CaSiO$_3$ perovskite: and once the required aluminium content is present, unexpected large amount of uranium (up to 35 wt.% UO$_2$) could be inserted into the lower mantle Ca-perovskite. Also we observed another interesting feature: the incorporation of uranium into the Al-CaSiO$_3$ ends up with saturation, since even with increased U and Al contents into the starting materials, no more than 35 wt.% UO$_2$ could be inserted into the Ca-perovskite. Such UO$_2$ content corresponds to a substitution of about 20% of Ca replaced by U, but more importantly this incorporation is allowed thanks to the substitution of nearly 40% of Si by Al: this latter feature could constitute a limit factor since Al is known to be about 34% bigger than Si when 6-fold coordinated. The distortion of the SiO$_6$ octahedra when Al replaces Si, could limit the coupled substitutions which then end up with saturation.

This study also showed that the high accuracy of the data obtained at the HP-XRD ID30 beamline (now ID27 beamline) at ESRF, allowed us to describe and to follow with temperature, the reaction of incorporation of uranium into the Al-CaSiO$_3$ perovskite. X-ray diffraction patterns collected as a function of temperature clearly evidenced the tetragonal distortion generated by the incorporation of U and Al into the Ca-perovskite. This incorporation occurs in parallel to the progressive intensity decrease of the peaks from the uraninite UO$_2$, which was the initial source of uranium. These XRD data collected in situ in a diamond anvil cell closely matched the data obtained from multi-anvil press experiments performed with the same starting assemblages: this indicates that, in spite of totally different heating modes (laser heating and furnace), these two HP techniques could definitively be complementary to study chemical reactions and associated crystal structure changes occurring at high pressures and high temperatures in deep mantle materials.

According to the present results, we can see that the aluminous CaSiO$_3$ perovskite has a high affinity for uranium. We could follow the evolution of the crystal structure of the U-bearing Al-CaSiO$_3$ perovskite until 54 GPa, which corresponds to a depth of about 1300 km (upper part of the lower mantle). Up to this pressure, we did not detect any sign of a possible further structural change: then we can assume that the tetragonal P4/mmm structure for this latter phase remains stable down to the base of the Earth's lower mantle. This work further confirmed that the Al–Ca-perovskite is able to incorporate an unexpectedly high content of uranium without any important structural change: this phase is then a candidate to host most or even all the uranium present in the deep Earth's mantle

(as discussed by Gautron et al. (2006)). In the case of the presence of Al–Ca-perovskite locally highly enriched in uranium, this latter phase could have an influence on the travel times of seismic waves, which could go through such material.

The crystal structure of the U-bearing Al-CaSiO$_3$ perovskite displayed new unexpected features. Unlike former studies that reported Al-bearing CaSiO$_3$ perovskites with lower compressibility, the U-bearing Al-CaSiO$_3$ perovskite is shown to have a higher compressibility than pure CaSiO$_3$ perovskite. A possible explanation could be given by the substitution of Ca by U which is about 13% smaller than Ca when located in a dodecahedron. Another noticeable difference is that the tetragonaly distorted U–Ca-perovskite, displays a c-axis longer than the a-axis, which is contrary to the results obtained for pure Ca-perovskite (Shim et al., 2002). This work reports a ratio c/a >1 at all pressures up to 54 GPa. This could be due to the replacement of some Si cations (in SiO$_6$ octahedra) by Al, which is 34% larger than Si when located in an octahedron, then generating a possible distortion preferentially along the c-axis. Coupled substitutions of CaSi$_2$ by UAl$_2$ are also expected to explain the change of the compression behaviour of c-axis relatively to a-axis, as described above in the results of this work. Note also that such coupled substitutions could contribute to stabilize the perovskite structure during the release of the pressure, leading it to be quenchable while other CaSiO$_3$ perovskites are known to bear a partial or complete amorphization upon decompression. It is up to now, the only occurrence of a crystalline Ca-bearing silicate perovskite recovered at room P and T conditions, which displays remarkable large grains up to 20–30 μm in size.

Another important implication of such U partitioning, is the correlated aluminium partitioning: in fact, because of its charge 3+, aluminium is known to have a strong influence on the iron partitioning (especially Fe^{3+} versus Fe^{2+}) between the two main mineral phases present in the lower mantle, the (Mg,Fe)SiO$_3$ perovskite and the (Mg,Fe)O magnesiowüstite. Local Al enrichment of the coexisting CaSiO$_3$ perovskite could then influence the Fe content of the (Mg,Fe) perovskite, and it is known that the iron content and oxidation state have a great effect on the chemical and physical properties of the (Mg,Fe)SiO$_3$ perovskite (Fiquet, 2001). Due to the relatively low uranium concentration expected in the Earth's mantle (McDonough and Sun, 1995), we can just imagine a scenario where uranium is locally and highly concentrated in the CaSiO$_3$ perovskite: because this incorporation is essentially related to that of aluminium, this could have an influence on the HP behaviour of the main mineral phase present in the deep mantle, the (Mg,Fe)SiO$_3$ perovskite.

Numerous previous studies have predicted that a deep source of primitive radiogenic material should be stored in the Earth's deep mantle (Becker et al., 1999; Helffrich and Wood, 2001; Albarède, 2005). Different shapes have been proposed to describe this source: small domains or blobs (less than 10 km large) rather present throughout the lower mantle (Albarède, 2005), a deep dense radiogenic layer present in the bottom half of the lower mantle (with a upper limit at 1600 km depth) (Kellogg et al., 1999; Van der Hilst and Karason, 1999), or hot and denser materials at the base of geographically localized big domes which have been observed in the deep lower mantle (Davaille, 1999; Davaille et al., 2005). Small domains are plausible but are under the detection limit of seismological techniques, while the deep layer has not been confirmed in spite of intense search to characterize the 1600 km depth discontinuity, which should be visible from seismic observations (Castle and Van der Hilst, 2003). The last observations and models of big domes could explain different features and arguments. Such models require a locally highly radioactive heat source to generate a bottom heating below the dome, and the material that could provide this heat could be the U-bearing Al-CaSiO$_3$ perovskite. After

preliminary experiments (paper in preparation), we can expect that thorium (which is the other important radioactive heat source in the Earth) behaves similarly to uranium: then the Al-CaSiO$_3$ is a candidate to be the only host of radioactive heat sources (U and Th) in the earth's mantle, and could provide the energy required for the existence and evolution of the big domes proposed to be present in the lowermost mantle.

References

Akber-Knutson, S., Bukowinski, M.S.T., Matas, J., 2002. On the structure and compressibility of CaSiO$_3$ perovskite. Geophys. Res. Lett. 29, 3, doi:10.1029/2001GL013523.

Albarède, F., 2005. The survival of mantle geochemical heterogeneities. In: Van der Hilst, R.D., Bass, J.D., Matas, J., Trampert, J. (Eds.), Earth's Deep Mantle Structure, Composition and Evolution. Am. Geophys. Union, Geophys. Monog. 160, 27–46.

Andrault, D., Fiquet, G., 2001. Synchrotron radiation and laser heating in a diamond anvil cell. Rev. Sci. Instrum. 72, 1283–1288.

Andrault, D., Neuville, D., Flank, A.M., Wang, Y., 1998. Cation sites in Al-rich MgSiO$_3$ perovskite. Am. Miner. 83, 1045–1053.

Asahara, Y., Ohtani, E., Kondo, T., Kubo, T., Miyajima, N., Nagase, T., Fujino, K., Yagi, T., Kikegawa, T., 2005. Formation of metastable cubic-perovskite in high-pressure phase transformation of Ca(Mg,Fe,Al)Si$_2$O$_6$. Am. Miner. 90, 456–457.

Becker, T.W., Kellogg, J.B., O'Connell, R.J., 1999. Thermal constraints on the survival of primitive blobs in the lower mantle. Earth Planet. Sci. Lett. 171, 351–365.

Béjina, F., Jaoul, O., Liebermann, R.C., 2003. Diffusion in minerals at high pressure: a review. Phys. Earth Planet. Int. 139, 3–20.

Caracas, R., Wentzcovitch, R.M., 2006. Theoretical determination of the crystal structure of CaSiO$_3$ perovskites. Acta Cryst. B62, 1025–1030, doi:10.1107/S0108768106035762.

Caracas, R., Wentzcovitch, R.M., Price, G.D., Brodholt, J., 2005. Equation of state and stability of CaSiO$_3$ under pressure. Geophys. Res. Lett. 32, 6, doi:10.1029/2004GL022144.

Castle, J.C., Van der Hilst, R.D., 2003. Searching for seismic scattering of mantle interfaces between 800 and 2000 km depth. J. Geophys. Res., doi:10.1029/2001JB000286.

Caussin, P., Nusinovici, J., Beard, D.W., 1988. Using digitized X-ray powder diffraction scans as input for a new PC AT Search/match program. Adv. X-ray Anal. 31, 423–430.

Corgne, A., Wood, B.J., 2002. CaSiO$_3$ and CaTiO$_3$ perovskite-melt partitioning of trace elements implications for gross mantle differentiation. Geophys. Res. Lett. 29, 1903, doi:10.1029/2001GL014398.

Corgne, A., Wood, B.J., 2004. Trace element partitioning between majoritic garnet and silicate melt at 25 GPa. Phys. Earth Planet. Inter. 143–144, 407–419.

Corgne, A., Allan, N.L., Wood, B.J., 2003. Atomistic simulations of trace element incorporation into the large site of MgSiO$_3$ and CaSiO$_3$ perovskites. Phys. Earth Planet. Inter. 139, 113–127.

Davaille, A., 1999. Simultaneous generation of hotspots and superswells by convection in a heterogeneous planetary mantle. Nature 402, 756–760.

Davaille, A., Stutzmann, E., Silveira, G., Besse, J., Courtillot, V., 2005. Convective patterns under the Indo-Atlantic "box". Earth Planet. Sci. Lett. 239, 233–252.

Fiquet, F., 2001. Mineral phases of the Earth's mantle. Z. Kristallogr. 216, 248–271.

Gautron, L., Madon, M., 1994. A study of the stability of anorthite in the *PT* conditions of the Earth's transition zone. Earth Planet. Sci. Lett. 125, 281–291.

Gautron, L., Kesson, S.E., Hibberson, W.O., 1996. Phase relations for $CaAl_2Si_2O_8$ (anorthite composition) in the system $CaO–Al_2O_3–SiO_2$ at 14 GPa. Phys. Earth Planet. Inter. 97, 71–81.

Gautron, L., Angel, R.J., Miletich, R., 1999. Structural characterisation of the high-pressure phase $CaAl_4Si_2O_{11}$. Phys. Chem. Miner. 27, 47–51.

Gautron, L., Greaux, S., Andrault, D., Bolfan-Casanova, N., Guignot, N., Bouhifd, M.A., 2006. Uranium in the Earth's lower mantle. Geophys. Res. Lett. 33, L23301, doi:10.1029/2006GL027508.

Gréaux, S., Farges, F., Gautron, L., Letard, I., Flank, A-M., Lagarde, P., 2007. Redox and speciation of uranium in Al-rich perovskites from high-pressure/high-temperature conditions. In: A.I.P. Conference Proceeding, X-Ray Absorption Fine Structure XAFS-13, 13rd International Conference, vol. 882, pp. 259–261.

Hammersley, A.P., Svensson, S.O., Hanfland, M., Fitch, A.N., Häusermann, D., 1996. Two-dimensional detector software: from real detector to idealised image or two-theta scan. High Press. Res. 14, 235–248.

Hammouda, T., 2003. High pressure melting of carbonated eclogite and experimental constraints on carbon recycling and storage in the mantle. Earth Planet. Sci. Lett. 214, 357–368.

Hanajiri, Y., Matsui, T., Arita, Y., Nagasaki, T., Shigematsu, H., Harami, T., 1998. EXAFS analyses of $CaTiO_3$ doped with Ce, Nd and U. Solid State Ionics 108, 343–348.

Helffrich, G.R., Wood, B.J., 2001. The Earth's mantle. Nature 412, 501–507.

Hirose, K., Nobumichi, S., Van Westrenen, W., Fei, Y., 2004. Trace element partitioning in Earth's lower mantle and implications for geochemical consequences of partial melting at the core-mantle boundary. Phys. Earth Planet. Inter. 146, 249–260.

Idiri, M., Le Bihan, T., Heathman, S., Rebizant, J., 2004. Behavior of actinide dioxides under pressure: UO_2 and ThO_2. Phys. Rev. B 70, 014113(1–8).

Irifune, T., 1994. Absence of an aluminous phase in the upper part of the Earth's lower mantle. Nature 370, 131–133.

Ita, J.J., Stixrude, L., 1992. Petrology, elasticity and composition of the mantle transition zone. J. Geophys. Res. 97, 6849–6866.

Jung, D.Y., Oganov, A.R., 2005. *Ab initio* study of the high-pressure behaviour of $CaSiO_3$ perovskite. Phys. Chem. Miner. 32, 146–153.

Kellogg, L.H., Bradford, H.H., Van der Hilst, R.D., 1999. Compositional stratification in the deep mantle. Science 283, 1881–1884.

Knittle, E., 1998. The solid/liquid partitioning of major and radiogenic elements at lower mantle pressures: implications for the core–mantle boundary region. In: Gurnis, M., Wysession, M.E., Knittle, E., Buffett, B.A. (Eds.), The Core–Mantle Boundary Region. Am. Geophys. Union, Geodyn. Ser. 28, 119–130.

Komabayashi, T., Hirose, K., Sata, N., Ohishi, Y., Dubrovinsky, L.S., 2007. Phase transition in $CaSiO_3$ perovskite. Earth Planet. Sci. Lett. 260, 564–569.

Kurashina, T., Hirose, K., Ono, S., Sata, N., Ohishi, Y., 2004. Phase transition in Al-bearing $CaSiO_3$ perovskite implications for seismic discontinuities in the lower mantle. Phys. Earth Planet. Inter. 145, 67–74.

Larson, A.C., Von Dreele, R.B., 1994. General Structure Analysis System (GSAS). Los Alamos National Lab. Rep. LAUR, 86–748.

Liu, L.-G., 1980. High-pressure phase transformations of fluorite-type dioxides. Earth Planet. Sci. Lett. 49, 166–172.

Liu, L.-G., 1982. Phase transformations in $MSiO_4$ compounds at high pressures and their geophysical implications. Earth Planet. Sci. Lett. 57, 110–116.

Liu, L.-G., Ringwood, A.E., 1975. Synthesis of a perovskite-type polymorph of $CaSiO_3$. Earth Planet. Sci. Lett. 14, 209–211.

Madon, M., Castex, J., Peyronneau, J., 1989. A new aluminocalcic high-pressure phase as a possible host of calcium and aluminium in the lower mantle. Nature 342, 422–424.

McDonough, W.F., Sun, S.-S, 1995. The composition of the Earth. Chem. Geol. 120, 223–253.

Pialoux, A., Touzelin, B., 1998. Study of U–Ca–O system by X-ray diffractometry at high temperature. J. Nuclear Mater. 255 (1), 14–25.

Poirier, J.-P., 2000. Introduction to the Physics of the Earth's Interior. Cambridge University Press, 312 pp., ISBN: 0-521-66392X.

Rubie, D.C., 1999. Characterising the sample environment in multi-anvil high-pressure experiments. Phase Transit. 68, 431–451.

Seitz, M.G., 1973. uranium and thorium diffusion in diopside and fluoroapatite. Carnegie Inst. Washington Yearb. 72, 586–588.

Shannon, R.D., 1976. Revised effective ionic radii and systematics studies of inter-atomic distances in halides and chalcogenides. Acta Cryst. A32, 751–767.

Shim, S.-H., Duffy, T., Shen, G., 2000a. The equation of state of $CaSiO_3$ perovskite to 108 GPa at 300 K. Phys. Earth Planet. Int. 120, 327–338.

Shim, S.-H., Duffy, T., Shen, G., 2000b. The stability and *P–V–T* equation of state of $CaSiO_3$ perovskite in the Earth's lower mantle. J. Geophys. Res. 105 (25), 955–25968.

Shim, S.-H., Jeanloz, R., Duffy, T.S., 2002. Tetragonal structure of $CaSiO_3$ perovskite above 20 GPa. Geophys. Res. Lett. 29, 2166, doi:10.1029/2002GL016148.

Stixrude, L., Cohen, R.E., Yu, R., Krakauer, H., 1996. Prediction of phase transition in $CaSiO_3$ perovskite and implications for lower mantle structure. Am. Miner. 81, 1293–1296.

Takafuji, N., Yagi, T., Miyajima, N., Sumita, T., 2002. Study on Al_2O_3 content and phase stability of aluminous-$CaSiO_3$ perovskite at high pressure and temperature. Phys. Chem. Miner. 29, 532–537.

Tarrida, M., Richet, P., 1989. Equation of state of $CaSiO_3$ perovskite to 96 GPa. Geophys. Res. Lett. 16, 1351–1354.

Toby, B.H., 2001. EXPGUI, a graphical user interface for GSAS. J. Appl. Cryst. 34, 210–213.

Tronnes, R.G., Frost, D.J., 2002. Peridotite melting and mineral-melt partitioning of major and minor elements at 22–24.5 GPa. Earth Planet. Sci. Lett. 97, 117–131.

Turcotte, D.L., Paul, D., White, W.M., 2001. Thorium–uranium systematics require layered mantle convection. J. Geophys. Res. 106, 4265–4276.

Van der Hilst, R.D., Karason, H., 1999. Compositional heterogeneity in the bottom 1000 kilometers of Earth's mantle toward a hybrid convection model. Science 283, 1885–1888.

Van Orman, J.A., Grove, T.L., Shimuzu, N., 1998. Uranium and thorium diffusion in diopside. Earth Planet. Sci. Lett. 160, 505–519.

Wang, Y., Weidner, D.J., Guyot, F., 1996. Thermal equation of state of $CaSiO_3$ perovskite. J. Geophys. Res. 101, 661–672.

Wood, B.J., Blundy, J.D., Robinson, A.C., 1999. The role of clinopyroxene in generating U-series disequilibrium during mantle melting. Geochim. Cosmochim. Acta 63, 1613–1620.

Yusa, H., Yagi, T., Shimobayashi, N., 1995. A new unquenchable high-pressure polymorph of $Ca_3Al_2Si_3O_{12}$. Phys. Earth Planet. Inter. 92, 25–31.

Zhang, J., Weidner, D.J., 1999. Thermal equation of state of aluminium-enriched silicate perovskite. Science 284, 782–784.